Impact of Oceanic Oscillations in Annual Trends of Precipitation Extremes in the Paraíba do Sul River Basin Assessed Based on the PSL Daily Gridded Precipitation Dataset

Mônica Carneiro Alves Senna (monicasenna@id.uff.br)
Universidade Federal Fluminense https://orcid.org/0000-0003-3236-1743
Gutemberg Borges França
Matheus Francisco Pereira
Mauricio Soares da Silva
Enio Pereira de Souza
Ian Cunha D'Amato Viana Dragaud
Lucio Silva de Souza
Nilton Oliveira Moraes
Vinicius Albuquerque de Almeida
Manoel Valdonel de Almeida
Maurício Nogueira Frota
Afonso Augusto Magalhães de Araujo
Karine do Nascimento Cardozo
Lude Quieto Viana

Research Article

Keywords: climate change, RClimDex, extreme climate indices, ENSO

Posted Date: March 16th, 2022

DOI: https://doi.org/10.21203/rs.3.rs-1389704/v1

Version of Record: A version of this preprint was published at Theoretical and Applied Climatology on April 22nd, 2023. See the published version at https://doi.org/10.1007/s00704-023-04451-y.

Abstract

The waters of the Paraíba do Sul River supply around 15 million people, most of whom live in metropolitan regions of the state of Rio de Janeiro. Climate change alters its precipitation regime and can cause an increase in the occurrence of extreme hydrological events. The variability of precipitation results from the combined effects of the surface conditions of the oceans and the variations in the dynamics of atmospheric systems. This work aims to detect possible changes in the climatic extremes of precipitation in the Paraíba do Sul hydrographic basin and to investigate evidences of correlation of these indices with the oceanic oscillations associated with the El Niño-Southern Oscillation, Pacific Decadal Oscillation, North Atlantic Oscillation and Atlantic Multidecadal Oscillation. Results indicate that the eastern and northeastern sectors of the basin present trends of increase in the total annual precipitation, in the number of very humid days and in the occurrence of extreme events, in a space of time up to five days. The west and southwest sectors, on the other hand, show decreasing trends in total annual precipitation, in the number of very humid days, but with an increase trend in the maximum amount of rainfall on five consecutive days. The central sector has characteristics of a transition zone. The correlation analyzes show that the majority of the oceanic oscillation indices have a very weak correlation with the extreme precipitation indices, while the wavelet transform does not indicate significant power at the low frequencies.

1. Introduction

In the past few decades, a considerable increase in the annual frequency of extreme weather events has been observed (*e.g.*, Marengo et al., 2007). This intensification has been attributed to human activities and climate change (Alexander et al., 2006; Carvalho et al., 2014; Ávila et al., 2020; Marengo et al., 2020). According to the Intergovernmental Panel on Climate Change (IPCC), there is strong evidence that the energy system used by today's society will have significant impacts on the climate due to the accumulation of greenhouse gases in the atmosphere, influencing future temperature and precipitation patterns throughout the globe (IPCC, 2018). These changes can lead to serious problems in vulnerable regions, particularly in sectors such as agriculture and water resources, which are already impacted by natural climatic variation, and can be intensified in a warmer climate and with possible changes in regional rainfall patterns (Chadwick et al., 2016; Zilli et al., 2017, Abou Rafee et al., 2020).

The waters of the Paraíba do Sul river supply approximately 15 million people, mostly from metropolitan regions in the state of Rio de Janeiro, which essentially depends on this hydrographic basin (Lopes, 2018; Ferreira, 2019; Brasiliense et al., 2020). These waters are also reallocated to the Cantareira System in order to mitigate the vulnerability of the main source of water of Metropolitan Area of São Paulo (Deusdará-Leal et al., 2020). Bearing in mind that the water cycle is directly linked to the climate, its changes —which alter the rainfall regime— can cause an increase in the occurrence of extreme hydrological events, such as floods and/or long periods of drought (Marengo and Alves, 2005; Teixeira and Satyamurti, 2011; Ribeiro, 2020). Groisman et al. (2005) showed that on a global scale, changes in intense rainfall tend to be more impacting than changes in average precipitation totals, and that

increases in events with extreme precipitation have occurred in many regions where no change in average totals or even a decrease in precipitation was observed.

Several regional studies have identified positive trends in rainfall extremes in southeastern Brazil (Dereczynski et al., 2013; Marengo et al. 2013; Carvalho et al. 2014; Avila et al. 2016; Zilli et al. 2017; Sobral et al., 2019; Ávila et al., 2020; Marengo et al., 2020). Ávila et al. (2016) found that the frequency and intensity of extreme daily precipitation have increased over mountainous regions in Rio de Janeiro state. Zilli et al. (2017) also found that the frequency of both rainy days and extreme daily precipitation events have increased in Sao Paulo state. However, precipitation has become more concentrated in fewer events in Rio de Janeiro and Espírito Santo states, both with positive trends in the intensity of extreme daily rainfall. Sobral et al. (2019) identified significant trends of annual rainfall increase in the northern Rio de Janeiro, and significant reduction trends in the mountainous and center-south regions of the state. Ávila et al. (2020) evidenced that consecutive dry days, maximum and heavy precipitation days are been observed more often in Viçosa-Minas Gerais. Marengo el at. (2020) showed a significant increase in the total volume of rainy-season rainfall during the last seven decades in the Metropolitan Area of São Paulo.

The variability of precipitation results from the combined effects of variations in the dynamics of atmospheric systems and the surface conditions of the oceans (Nobre and Shukla, 1996; Luiz-Silva et al., 2020). The South American continent is located between the two largest oceans, the Pacific and the Atlantic. Therefore, understanding the phenomena that occur in these oceans and their respective atmospheric couplings is of fundamental importance for studies of the dynamics of precipitation in the region (Siqueira, 2012).

Marengo (2006) carried out a study for the period 1979–2000, and have found reductions in precipitation, runoff and moisture convergence in El Niño years, and increases in these variables in La Niña years in northern South America, including northeastern Brazil. The South Region of Brazil presents the opposite behavior of what occurs in the North and Northeast, that is, during El Niños (La Niñas), the rate of precipitation increases (decreases) over this region. El Niño and La Niña events do not directly increase or reduce precipitation in southeastern Brazil (Minuzzi et al. 2006, 2007; Cataldi et al., 2010; Brito et al., 2017; Oliveira-Júnior et al., 2018; and Sobral et al. 2019).

Cardoso and Cataldi (2012) observed that the flow of Brazilian rivers has significant relationships with different climatic and teleconnection patterns, with emphasis on the correlation with the lower frequency variability patterns, such as Pacific Decadal Oscillation (PDO). Changes in atmospheric circulation modes, associated with PDO in South America, are characterized by the strengthening of Walker circulation during the cold phase of PDO and by its weakening during the hot phase (Garcia and Kayano, 2008). Kayano and Andreoli (2007) point out that the influence of El Niño-Southern Oscillation (ENSO) through teleconnections, over the precipitations in South America are considered strong when ENSO and PDO are in the same phase, creating constructive effects. Otherwise, opposite phases the result is destructive.

Capozzoli et al. (2017) characterized the main patterns of spatial and temporal variability of river flows in the main Brazilian hydrographic basins, relating them to climatic patterns through Principal Component Analysis. The main flow modes of the rivers presented interannual variations associated with the ENSO phenomenon and significant correlations with the sea surface temperature (SST) in the tropical Atlantic. Climatic patterns associated with the multidecadal variability of the Atlantic Ocean and the decadal of the Pacific Ocean, have persistent relationships with the first six flow modes.

Several studies have shown the existence of variability in the interdecadal scale in precipitation in Argentina and Uruguay, and in river flows in southeastern South America (Castañeda and Barros, 1994; Krepper and Sequeira, 1998; Robertson and Mechoso, 1998). Santos et al. (2011) showed that the positive phase of the North Atlantic Oscillation (NAO) significantly affects the tropical region, inhibiting convection along the Intertropical Convergence Zone (ITCZ) and intensifying upward movements in northern South America.

It is known that precipitation over the tropical Atlantic is shifted northwards during the warm phase of the Atlantic Multidecadal Oscillation (AMO); this implies an anomalous position of the ITCZ to the north, which decreases precipitation during the rainy season in the north of the Brazilian Northeast, from March to May (Knight et al., 2005). However, the sequence of the AMO cycle can reverse this signal by forcing the ITCZ to the south and, thus, oscillating between drier and wetter decades (Knight et al., 2005). When analyzing sedimentary data from the Rio da Prata Basin, Chiessi et al. (2009) found a periodicity of 64 years linked to the South Atlantic Convergence Zone (SACZ) and the monsoons in South America, which was attributed to AMO. Thus, the cold phase of AMO (hot phase of AMO) corresponds to a warmer South Atlantic (cold), which increases (decreases) the activity of the SACZ also due to the position of the Intertropical Convergence Zone (ITCZ), and displaces the main precipitation band of the South America monsoon to south (north).

The Paraíba do Sul River Basin is located in an intermediate area between the regions that present strong and opposite signs of these oceanic oscillations in their precipitation regimes. Thus, the objective of this study is to identify possible changes in the precipitation extremes for the Paraíba do Sul river basin and to investigate, as successfully described in the work of Zilli et al. (2017), the correlation of the PSL Daily Gridded Precipitation Dataset – a set of pure precipitation observational data – with ocean oscillations El Niño-Southern Oscillation (ENSO), Pacific Decadal Oscillation (PDO), North Atlantic Oscillation (NAO) and Atlantic Multidecadal Oscillation (AMO).

2. Material And Methods

2.1. Study area

The Paraíba do Sul river basin (Fig. 1) covers three states in the Southeast Region of Brazil and has a drainage area of approximately 55,500 km², between the parallels 20º 26' S and 23º 00' S and between the meridians 41º 00' W and 46º 30' W. It is limited to the North by the basins of the rivers Grande and

Doce and by the mountains of Mantiqueira, Caparaó and Santo Eduardo. To the Northeast, the Itabapoana River basin establishes the limit of the basin. To the south, the limit is formed by the São Paulo and Fluminense stretches of Serra do Mar (CEIVAP, 2006). The Paraíba do Sul River rises in the Serra da Bocaina, in the state of São Paulo, at 1,800 m altitude, and flows into the North Fluminense Region, in the municipality of São João da Barra, covering an approximate length of 1.15 thousand km.

The rainfall presents itself with two very characteristic periods: a dry season (from June to August), characterized by tropical conditions of continental nature, with low relative humidity of the air, and a rainy season (from October to March), characterized by the domain of the mass of humid and unstable equatorial continental air, with high relative humidity and high levels of precipitation (ANA, 2010). In addition to these two well-defined seasons, there are transition periods: from the dry to the wet season (September and October) and from the wet to the dry season (April and May). The annual precipitation varies from 1000 mm over the northern part of the Rio de Janeiro state and 2000 mm over the Mantiqueira mountains. About 80% of the rainfall occurs in the months of October through March, suggesting a monsoon-like regime (Brasiliense et al., 2020).

According to Nimer (1989), the factors that act on the intensity and distribution of precipitation in this region can be classified as static and dynamic. Among the static ones, the following stand out: the rugged topography, which favors precipitations, as it increases air turbulence due to orographic ascension; the latitudinal position, which, by receiving strong solar radiation, provides better conditions for evaporation; and its position at the western edge of the ocean, which is influenced by the proximity to the coastal environment and favors the existence of condensation nuclei stimulating the formation of clouds. Dynamic factors are atmospheric mechanisms that interfere with static factors. Among the main players are the South Atlantic Subtropical Anticyclone (SASA), the South Atlantic Convergence Zone (SACZ), the frontal systems (FS), the instability lines (IL), the mesoscale convective systems (MCS) and breezes (Brito et al., 2017). According to Dereczynski et al. (2009), among these meteorological systems, the most influential in the rainfall regime are FS during winter and SACZ during summer time.

Brasiliense et al. (2017) analyzed the characteristics of an event of intense rains that occurred in the Paraíba do Sul River Basin. This event was related to the configuration of an episode of SACZ, which lasted eight days, after the arrival of a cold front in the state of São Paulo. There was convergence over southeastern Brazil, the flow of moisture from the south of the Amazon and the tropical South Atlantic, providing large amounts of moisture for convective activity. The most notable aspect of this event was the development of a cyclonic vortex embedded in the SACZ, over the Atlantic Ocean, with a hot core in the lower troposphere and a cold core at higher levels, which intensified the rains in the study region.

2.2. Precipitation data

Precipitation databases based on meters of good quality and sufficient density provide a reliable estimate of precipitation in a given area. Due to the lack of daily and reliable historical series of easy access, many scientific works have been using regular grid data sets derived from surface stations (*e.g.*,

Liebmann and Allured, 2005; Zilli et al., 2017). A grid precipitation database has the advantage of allowing general analysis of regional patterns and, on a large scale, precipitation trends.

In this study, the Physical Sciences Laboratory (PSL) South America Daily Gridded Precipitation database was used, which provides data on grid precipitation and daily frequency, covering the period between 1938 to 2012, with spatial horizontal resolution of 0.5º x 0.5º latitude-longitude, based on the precipitation observed in stations located in South America (Liebmann and Allured, 2005). The dataset is comprised of daily totals of precipitation from all valid stations within a sample radius of 0.5 from the grid point's center (Zilli et al., 2017). This ensures the inclusion of all stations in at least one grid point (Liebmann and Allured, 2005). According to Liebmann and Allured (2005), the PSL daily grid precipitation dataset has varied station density, ranging from 8 to 67 stations per grid point in the study area, and has three limitations: (1) A few stations may be included in up to four distinct grid points, producing further smoothing; (2) Spatial smoothing hides out extreme precipitation with a spatial scale smaller than the grid resolution; (3) The exclusion of suspiciously huge values in the station data can produce a low bias in the related grid point. In Brazil, the main sources that compose this data are: Electric Energy Companies, National Water and Basic Sanitation Agency (ANA), National Meteorological Institute (INMET) and specialized state agencies. The PSL dataset was chosen because it had a long daily gridded precipitation available data for our region. Zilli et al. (2017) compared the patterns identified for this dataset to individual stations and discovered good general agreement. The data were obtained at https://www.esrl.noaa.gov/psd/data/gridded/ data.south_america_precip.html.

Using the NCL (NCAR Command Language) scripts were prepared to cut the precipitation data only within the Shapefile of the Paraíba do Sul river basin (made available by the concessionaire LIGHT Energia S.A). Then, the precipitation time series of each of the 19 grid points within the study region (Fig. 1) were analyzed, looking for spurious data, and all values above 100 mm were checked manually. No data needed to be excluded as these were days with intense rainfall occurring in neighboring areas and/or with rain occurring in the previous or subsequent days. Then, the percentage of missing data was obtained in relation to the total time series, which was less than 0.5%. Therefore, none of the grid points needed to be removed. The 19 grid points (Fig. 1) correspond to different cities in the states of Minas Gerais, Rio de Janeiro and São Paulo, but only one city per grid was selected to guide a more detailed discussion of the results obtained (Table 1).

Table 1
City corresponding to each grid point

Grid Point	Correspondent City
1	Muriaé (MG)
2	Itaperuna (RJ)
3	Santos Dumont (MG)
4	São João Nepomuceno (MG)
5	Recreio (MG)
6	Cambuci (RJ)
7	Cardoso Moreira (RJ)
8	Bom Jardim de Minas (MG)
9	Belmiro Braga (MG)
10	Chiador (MG)
11	Duas Barras (RJ)
12	Cruzeiro (SP)
13	Resende (RJ)
14	Pinheiral (RJ)
15	São Francisco Xavier (SP)
16	Taubaté (SP)
17	Cunha (SP)
18	Santa Branca (SP)
19	Natividade da Serra (SP)

Figure 1 - Paraíba do Sul river basin (delimited by a blue line), and its 19 grid points referring to the precipitation database used. The yellow grid points represent the northeast areas (1 to 7 and 9 to 11), the pink one the northwest (8), and the red points the southwest areas of the basin (12 to 19).

2.3. Indices of climatic extremes of precipitation

In the search for a methodology that serves as an analysis of climate change, the World Meteorological Organization (WMO) created a working group that built indices for monitoring and detecting climate change. This group developed a software called RClimDex, which provides a friendly interface for the calculation of extreme weather indices. Several researchers such as Silva and Azevedo (2008), Santos et

al. (2009), Souza and Azevedo (2012), Silva and Dereczynski (2014), Valverde and Marengo (2014), Oscar Jr. (2015), Regoto et al. (2018) have used the tool to monitor climate trends in several states in Brazil. RClimDex is based on the computational language R and on an electronic spreadsheet, and presents the indices estimated through figures and spreadsheets, in addition to statistical information, such as linear trend calculated by the least squares' method; level of statistical significance of the trend, obtained through the *t-student* test (p-value); coefficient of determination (R^2 in percentage) and standard error of estimate (Zhang and Yang, 2004). The calculated p-value represents the level of statistical significance (if the *p-value* of any index is equal to or less than 0.1, the trend of the index is statistically significant by 90%; if it is equal to or less than 0.05, in 95% and, for p less than 0.01, the trend has 99% statistical significance).

In this study, of the twenty-seven climate change detection indices produced by RClimDex (Zhang and Yang, 2004), only those referring to precipitation data were used. Table 2 summarizes the trends and Interannual variability of extreme indices considered in this work.

Table 2
Definition of the climatic extremes of precipitation used in this study

(Source: http: //etccdi.pacificclimate.org/list_27_indices.shtml).

Index	Index definition	Unit
RX1day	Maximum 1-day precipitation	mm
RX5day	Maximum consecutive 5-day precipitation	mm
SDII	Simple precipitation intensity index	$mm.day^{-1}$
R10	Count of days for precipitation ≥ 10mm	day
R25	Count of days for precipitation ≥ 25 mm	day
CDD	Consecutive dry days (Maximum number of consecutive days with daily precipitation < 1 mm)	day
CWD	Consecutive wet days (Maximum number of consecutive days with daily precipitation ≥ 1 mm)	day
R95p	Very wet days (Daily precipitation amount > 95th percentile)	mm
R99p	Extremely wet days (Daily precipitation amount > 99th percentile)	mm
PRCPTOT	Wet-days annual amount	mm

2.4. Ocean oscillation indices

The El Niño-Southern Oscillation (ENSO) is characterized by the Southern Oscillation Index (SOI), defined as the difference between normalized deviations of atmospheric pressure at sea level between the following Pacific Ocean regions: Tahiti (17º S; 150º W), in French Polynesia, and Darwin (12º S; 130º E), in northern Australia. The negative phase of the SOI represents below-normal air pressure at Tahiti and above-normal air pressure at Darwin. Prolonged periods of negative (positive) SOI values coincide with abnormally warm (cold) ocean waters across the eastern tropical Pacific typical of El Niño (La Niña) episodes. The SOI monthly time series was obtained from the NOAA (National Oceanic and Atmospheric Administration) website at: https://www.ncdc.noaa.gov/teleconnections/enso/indicators/soi/. The period available is from 1951 to the present.

The Pacific Decadal Oscillation (PDO) has been commonly represented by the PDOI, which is the PDO Index. The PDOI is defined as the first major component of sea surface temperature (SST) anomalies in the North Pacific, between latitudes 20° N and 90° N, with the withdrawal of the climate trend. When SSTs are anomalously cool in the interior North Pacific and warm along the Pacific Coast, and when sea level pressures are below average over the North Pacific, the PDOI has a positive value. When the climate anomaly patterns are reversed, with warm SST anomalies in the interior and cool SST anomalies along the North American coast, or above average sea level pressures over the North Pacific, the PDOI has a negative value. The PDOI monthly time series was obtained from the NOAA website at: https://www.ncdc.noaa.gov/teleconnections/pdo/. The period available is from 1854 to the present.

The North Atlantic Oscillation (NAO) is represented by an index given by the difference in atmospheric pressure, at sea level, between Iceland and the Azores (NAOI). The positive phase of the NAOI reflects below-normal heights and pressure across the high latitudes of the North Atlantic and above-normal heights and pressure over the central North Atlantic, the eastern United States and western Europe. The negative phase reflects an opposite pattern of height and pressure anomalies over these regions. The NAOI monthly time series was obtained from the NOAA website at: https://www.ncdc.noaa.gov/teleconnections/nao/. The period available is from 1950 to the present.

The Atlantic Multidecadal Oscillation (AMO) is characterized by an index (AMOI), which considers the SST anomalies in the northern Atlantic region and the Gulf of Mexico region. After this initial calculation between 0º and 70º north, the data is standardized using the SST climatology. Prolonged periods of negative (positive) AMOI values represent below-normal (above-normal) SSTs in the North Atlantic Ocean. The AMOI monthly time series was obtained from the NOAA website at: https://www.esrl.noaa.gov/psd/data/timeseries/AMO/. The period available is from 1856 to the present.

2.5. Correlation between rates of oceanic oscillations and precipitation extremes

The calculation of the correlations between the extreme climatic precipitation indices and the oscillation indices of the Atlantic and Pacific Oceans was done using Pearson's correlation coefficient (r), efficient to estimate the degree of relationship between any variables. Pearson's correlation coefficient varies from −1 to 1. The sign indicates a positive or negative direction of the relationship and the value suggests the

strength of the relationship between the variables. A perfect correlation (-1 or 1) indicates that the score of one variable can be determined exactly by knowing the score of the other. On the other hand, a zero-value correlation indicates that there is no linear relationship between the variables. Table 3 shows the different classes with the correlation values between the variables and their interpretations.

Table 3
Values and interpretation of the correlation coefficients (Hinkle et al., 2003).

Correlation Values (module)	Interpretation
0.00 a 0.19	Very weak correlation
0.20 a 0.39	Weak correlation
0.40 a 0.69	Moderate correlation
0.70 a 0.89	Strong correlation
0.90 a 1.00	Very strong correlation

2.6. Wavelet transform

In order to decompose the one-dimensional precipitation time series in the double time-frequency domain, thus allowing the identification of the main modes of variability and their variations in time, the wavelet transform was used (Torrence and Compo, 1998; Morettin, 1999; Vitorino et al., 2006; Echer et al., 2008). The wavelet analysis was used according to the methods presented in Torrence and Compo (1998), with bias rectification following the method proposed by Liu et al. (2007). Given the frequent use in the analysis of geophysical data (Liu et al., 2007), Morlet's wavelet was chosen as the basic function of the wavelet. The time average of the power was calculated for the entire local spectrum, producing the global spectrum of the wavelet (Torrence and Compo, 1998). Morlet's wavelet is defined as a complex exponential wave, modulated by a Gaussian, described by the following expression:

$$\psi_0(\eta) = \pi^{-1/4} e^{i\omega_0\eta} e^{-\eta^2/2} \quad (1)$$

In this expression, $\psi_0(\eta)$ is the value of the wavelet in the dimensionless time η, and ω_0 is the dimensionless frequency, equal to 6 in this study to satisfy an admissibility condition; i.e., the function must have zero mean and be located in the space of time and frequency to be “admissible” like a wavelet (Torrence and Compo, 1998). For these calculations, scripts were developed in Python language.

This approach of using the wavelet in precipitation data has already been applied in other studies, and allows to associate the existing variability with atmospheric and oceanic processes (*e.g.*, Costa et al., 2016; Adepitan and Falayi, 2019).

3. Results And Discussion

This section discusses (i) the spatial distribution of rainfall trends, (ii) the correlation between rates of oceanic oscillations and precipitation extremes and (iii) the wavelet technique in order to verify the possible existence of different frequency patterns from the investigated correlations.

3.1. Spatial distribution of rainfall trends

Figure 2 illustrates examples of trend curves for the SDII index of the following cities located in the Paraíba do Sul basin: Muriaé, Itaperuna, Cambuci and Recreio, in the period from 1938 to 2011. Different trends are observed before and after the beginning of the 1980s, and changes in the trends of climatic precipitation indices during the 1980s, especially those referring to extreme precipitation (RX1day, R95p, R99p), have been identified in several studies (eg: You et al. (2011), in China; Longueville et al. (2016), in Burkina Faso; Donat et al. (2016) and Dong et al. (2021), in different parts of the globe). The studies by Min et al. (2011), Zhang et al. (2013), Donat et al. (2016) and Dong et al. (2021) indicate that the increase in the extremes of precipitation can be attributed to anthropic actions, associated with the increasing emission of greenhouse gases. Teixeira and Satyamurty (2011) find a reduction in the number of heavy rainfall events in southeastern Brazil after the beginning of the 1980s, but they do not investigate the cause of this behavior. In this region, precipitation can be especially affected by position and intensity of the SACZ and the SASA, and during 1960–2019 the SASA has intensified and slightly moved southwestward of its normal position (Reboita et al., 2019; Marengo et al., 2020). This change influences the transport of humidity and therefore impact precipitation.

Figure 2. Linear (solid line) and non-linear (dashed line) trends of the SDII index, whose locations are indicated in Figures (2a – 2d), from 1938 to 2011.

The images (a) to (j) of Figs. 3 illustrate the spatial distribution of the trends of extreme climatic precipitation indices, described in Table 2, obtained in the Paraíba do Sul basin, from 1982 to 2011 (data do not reflect the complete time series, considering the trends observed in Fig. 2). Symbols in the form of a full triangle (in red or blue) indicate statistically significant trends (greater than 90% confidence) and the position of the apex of the triangle indicates a positive (upward) or negative (downward) trend.

In general, the eastern and northeastern sectors of the Paraíba do Sul river basin have positive trends in the PRCPTOT index, as shown in Fig. 3a, with emphasis on the region around the of municipality of Itaperuna, with a statistically significant trend of 8.6 mm/year. The west and southwest regions show the opposite, negative PRCPTOT trends, with the region around Santa Branca standing out, also with a statistically significant trend of -9.3 mm/year. The results for the central region indicate a transition zone pattern, since there are alternations between null trends, positive or negative, all without statistical

significance. Sobral et al. (2019) also identified significant trends of rainfall increase in northeastern sectors of the Paraíba do Sul river basin, probable because this region is greatly influenced by Serra do Mar and Mantiqueira ridges, in the SW/NE direction (Brito et al., 2017). Besides, Reboita et al. (2019) indicate that the area of the SASA shows an expansion southward and westward of its normal position, and this expansion can shift dry zones southward.

The CDD index featured in Fig. 3b shows, in general, negative trends in the central sector of the basin, mainly in the region of the city of Resende, with a value of -0.6 days/year with statistical significance. In the east and northeast regions there are some points with a positive trend in the CDD index, among which the Chiador and Cambuci cities stand out, with 0.3 and 0.4 days/year, respectively. Both points with statistical significance of CDD trend values. In the west and southwest regions, there were varied trends, all without statistical significance.

In Fig. 3c, negative and null trends of the CWD index are identified in most of the region, except for two areas with an increase in CWD (in the municipalities of Cunha and São João Nepomuceno). In the central region, the trends of the referred index are mostly negative, while the northeast and southwest regions do not indicate a trend. Among the localities analyzed, the Santa Branca region deserves to be highlighted, as it presents statistical significance with a negative CWD trend of 0.6 days/year. This reduction in CWD can also be related to the southwestward expansion of SASA found in many studies (Reboita et al., 2019; Carpenedo and Ambrizzi, 2020; Marengo et al., 2020).

Figure 3d shows the positive trend of the R10 index in some regions of the northeast of the basin, with emphasis on the municipality of Itaperuna, whose statistical significance ensures reliability as to the increase of 0.4 days/year. As already documented in Fig. 3a, this same region also showed statistical significance for the positive trend of PRCPTOT index. In the southwest sector are concentrated some regions with a negative trend of R10, but none with statistical significance. In the central region, on the other hand, there is a variation between areas with zero trends and negative trends for the same index.

Analyzing the R25 index in Fig. 3e, it can be seen that the eastern and northeastern sectors of the basin concentrate areas with a positive R25 trend, four of them with statistical significance. Such regions are: Muriaé, Itaperuna, Cambuci and Duas Barras, with trends of around 0.2 days/year. In the western and central sectors, there are null trends in most points. In the southwest sector, null trends are observed, alternating with a few regions with a negative trend in R25, but all without statistical significance.

Figure 3f illustrates the behavior of the R95p index (very humid days), observing positive trends in most of the basin, especially in the central, east and northeast regions. It is worth mentioning that the R95p trends have statistical significance for the regions located in the municipalities of Muriaé, Itaperuna, Cambuci, Cardoso Moreira and Duas Barras, with trend values equal to 8.5, 5.5, 6.5, 4.1 and 5.9 mm/year, respectively. The west and southwest sectors show negative trends in the R95p index, but without statistical significance.

Figure 3g illustrates the spatial distribution of the trend of the R99p index. It is noted that in the east and northeast regions there is a variation between null and positive trends in extremely humid days. The regions in the vicinity of Cambuci and Duas Barras stand out, whose R99p trends are statistically significant with their values equal to 3.2 and 4.2 mm/year, respectively. In the central region, values of negative and positive trends of R99p are observed, but the Pinheiral region differs from the others, as it presents a R99p trend of 3.2 mm/year with statistical significance. For the western region and for the regions of the municipalities of Santa Branca and Natividade da Serra, to the southwest, values with null and negative trends are identified, respectively.

For the RX1day index, as shown in Fig. 3h, it is observed that only one area has a negative trend, located in Santos Dumont, northern region of the basin. In the northeast and east regions, positive trends of RX1day are identified, with emphasis on Cardoso Moreira and Duas Barras, with statistically significant trend values of 0.5 and 0.9 mm/year, respectively. In the central and southwest sectors, trend values of RX1day are found, ranging from null to positive, but without statistical significance.

Figure 3i shows the spatial distribution of trends in the RX5day index. It is noted that there is a predominance of positive trend of RX5day in most of the region, except in four locations with negative trends and in two neutral or null, all associated with indices without statistical significance. In the east, northeast, west and southwest regions, there are positive trends of RX5day, with emphasis on municipalities of Muriaé, Itaperuna, Cambuci, Cardoso Moreira, Duas Barras and Cunha, whose data exhibit trends with statistical significance of 1.4, 2.0, 1.4, 2.3, 1.3 and 1.3 mm/year, respectively.

The SDII index graph shown in Fig. 3j shows null trends across the Paraíba do Sul River basin. In the northeast region, SDII trends with statistical significance occur in Muriaé, Itaperuna, Cambuci and Cardoso Moreira regions.

(a) PRCPTOT	(b) CDD
(c) CWD	(d) R10
(e) R25	(f) R95p
(g) R99p	(h) RX1day
(i) RX5day	(j) SDII

Figure 3 – Spatial distribution of trends in the PRCPTOT index [mm/year] (a), CDD [day/year] (b), CWD [day/year] (c), R10 [day/year] (d), R25 [day/year] (e), R95p [mm/year] (f), R99p [mm/year] (g), RX1day [mm/year] (h), RX5day [mm/year] (i), and SDII [mm/day] (j) for the period from 1982 to 2011 in the Paraíba do Sul river basin.

The spatial distributions of the trends in the extreme precipitation indices showed some distinct characteristics of the sectors of the Paraíba do Sul River basin. The east and northeast regions have the largest number of areas with statistically significant trends of the considered indices. The trends associated with these regions, in general, reflect an increase in total annual precipitation (PRCPTOT

index), very humid days (R95p), maximum amount of precipitation in 1 day (RX1day) and in the maximum amount of precipitation in 5 consecutive days (RX5day). According to Reboita et al. (2009), during positive phase of the Southern Annular Mode (SAM) there are positive anomalies of precipitation over the northern part of South America because the SACZ is displaced northward from its climatological position, and a positive SAM phase trend is observed since 1993. Less generally, some regions show positive trends in the maximum number of consecutive dry days (CDD) and in the number of days with rainfall above 25 mm (R25). The increase in the number of consecutive dry days, together with the combination of the other trends mentioned, indicate a possible climate change as intense precipitation is concentrated in few days, separated by longer dry spells, the same result was identified by Zilli et al. (2017) in Rio de Janeiro state and Marengo et al. (2020) in Metropolitan Area of São Paulo.

The central region presents characteristics of a transition zone for some indices, such as the trend in the distribution of annual rainfall shown in Figure 3a, and in the maximum amount of precipitation in 5 consecutive days, shown in Figure 3i. In this sector, heterogeneous tendencies of the studied indices are verified, being just a few cases with statistical significance. However, it is noted, not only a reduction in the maximum number of consecutive dry days (CDD), but also a reduction in the maximum number of consecutive wet days (CWD). In addition, a positive trend is identified for very humid days (R95p) and extremely humid days (R99p). On the other hand, a negative trend in the maximum amount of precipitation in 5 consecutive days (RX5day) is an indicative of larger accumulation occurring in fewer rainy days, similar trends were identified by Dereczynski et al. (2013) and Zilli et al. (2017) in Rio de Janeiro.

For the west and southwest regions, there were also few indices with statistical significance. In general, the PRCPTOT index confirms a negative trend in total annual precipitation. The R95p index indicates a decrease in very humid days while the RX5day index shows a positive trend in the maximum amount of precipitation in 5 consecutive days. The regions in the vicinity of the municipalities of Santa Branca and Cunha have more striking trends, some quite distinct from each other. Near Santa Branca, negative trends are identified in total annual precipitation (PRCPTOT index), in the maximum number of consecutive wet days (CWD), in the number of days with precipitation above 10 mm (R10), as well as in the number of days with precipitation above 25 mm (R25). This may be related to the southwestward expansion of SASA previously cited (Reboita et al., 2019; Carpenedo and Ambrizzi, 2020; Marengo et al., 2020) and marks, quite clearly, the difference in its precipitation distribution when compared with areas in the northeast region. The region around Cunha differs from the others, in particular because it is the only one that has a positive trend in the total annual precipitation (PRCPTOT), both in the maximum number of consecutive wet days (CWD) and in the very wet days index (R95p). Most likely, such differentiation can be attributed to some local factor specific to the area, such as topography.

Negative precipitation anomalies over southeastern Brazil, especially during the summer, may be related to the displacement of the SASA to the west of its climatological position, acting as an atmospheric block and preventing the propagation of transient systems (see Coelho et al., 2015; Reboita et al., 2015). The position and intensity of SASA can be affected by Southern Annular Mode (SAM). That is, when it is in

the positive phase, it has negative (positive) geopotential height anomalies in the high (medium) southern latitudes, associated with the anomalous displacement of the SASA and ITCZ to the south. The opposite occurs during the negative phase of the SAM (Sun et al., 2017; Carpenedo and Ambrizzi, 2020). Other studies show a tendency for a greater number of occurrences of the positive phase of SAM in the last decades, mainly due to the increase in the concentration of greenhouse gases (Fyfe et al., 1999; Kushner et al., 2001; Stone et al., 2001; Cai et al., 2003; Marshall et al., 2004). With SASA and ITCZ positioned further south, precipitation deficits occur over central-southern Brazil and increases in precipitation in the North and Northeast (Carpenedo and Ambrizzi, 2020).

In addition, the results found agree with those obtained by Ferreira (2019), who observed an increase in the PRCPTOT, RX5day, R20 and SDII indices in the northeast portion of the Paraíba do Sul river basin, and a decrease in these same indices in the central and southwest portion of the basin. Recent studies show an increase in the accumulated precipitation in extreme rain events and its higher frequency of occurrence (Ávila et al., 2016; Zilli et al., 2017; Regoto et al., 2018; Ávila et al., 2020; Marengo et al. 2020). A similar result was found in this work, since, for the most part, the trends with statistical significance refer to the maximum amount of precipitation in 5 consecutive days, to very humid days and to the number of days with precipitation above 25 mm (corresponding to the indices RX5day, R95p and R25), mainly in the northeast side of the basin. On the other hand, the decrease in consecutive wet days (CWD) predominates, indicating a non-homogeneous distribution of rainfall throughout the year.

3.2 Correlation between rates of oceanic oscillations and precipitation extremes

The correlation coefficients between each extreme precipitation index and each ocean oscillation index in the period from 1938 to 2011 are shown in Tables 4 and 5. The entire available sample period was used, because when the sample size is small, the value Pearson's linear correlation coefficient must have a high magnitude to be meaningful, and the sample may not be representative of the population (Hair et al., 2005). The values of the correlation coefficients considered weak are highlighted in blue and, in red, those considered moderate, following the previously established criteria (Table 3). Most ocean oscillation indices had a very weak correlation with precipitation indices for most of the 19 grid points, indicating that precipitation in the Paraíba do Sul river basin is not dependent of these ocean oscillations in a strongly way. The only exception was the correlation between SOI (Southern Oscillation Index) and the CDD (Consecutive Dry Days), whose values fall into the weak and moderate categories, for most of the basin (12 of the 19 grid points). The highest value of the correlation coefficient found between these two indices was 0.41 in the Chiador city. In addition, all the correlations between SOI and CDD were positive, indicating that these indices are directly proportional. This implies that positive SOI values, which correspond to the La Niña phenomenon, can increase the number of consecutive dry days in the region, while negative SOI values, associated with El Niño, can decrease the number of consecutive dry days.

Table 4 - Correlation data between the oceanic oscillation indices (SOI, PDOI, NAOI and AMOI) and the climatic precipitation indices (CDD, CWD, PRCPTOT, R10 and R25).

CDD - Consecutive Dry Days

	A1	A2	A3	A4	A5	A6	A7	A8	A9	A10	A11	A12	A13	A14	A15	A16	A17	A18	A19
SOI	0.29	0.25	0.23	0.21	0.31	0.27	0.21	0.35	0.22	0.41	0.12	0.14	0.19	0.22	0.08	0.14	0.05	0.24	0.01
PDOI	-0.09	0.01	-0.14	-0.21	-0.14	-0.14	-0.06	-0.28	-0.21	-0.23	0.03	-0.21	-0.15	-0.11	-0.15	-0.08	0.06	-0.16	-0.15
NAOI	-0.09	-0.05	-0.09	-0.10	-0.08	-0.19	-0.07	-0.05	-0.07	-0.21	-0.03	-0.07	-0.08	-0.14	-0.02	-0.08	0.03	0.05	0.08
AMOI	-0.06	-0.04	0.08	0.02	0.09	0.18	0.07	-0.04	-0.10	0.11	0.23	0.10	-0.14	0.00	0.02	0.03	0.06	0.04	0.02

CWD - Consecutive Wet Days

	A1	A2	A3	A4	A5	A6	A7	A8	A9	A10	A11	A12	A13	A14	A15	A16	A17	A18	A19
SOI	-0.12	0.03	-0.12	0.14	0.02	-0.08	0.09	-0.06	-0.06	-0.27	-0.16	-0.10	-0.13	-0.06	0.01	0.03	0.05	-0.14	-0.01
PDOI	-0.06	-0.16	-0.10	-0.03	-0.14	0.01	-0.14	-0.11	-0.07	0.04	-0.06	0.00	-0.09	-0.13	-0.10	-0.15	-0.13	0.07	-0.17
NAOI	0.10	-0.01	-0.01	-0.02	0.07	-0.14	-0.08	-0.05	0.10	0.06	0.19	0.15	0.11	0.02	0.04	0.16	0.10	0.14	-0.02
AMOI	0.01	0.03	0.08	0.02	0.05	0.05	0.01	0.03	-0.06	-0.26	-0.17	0.03	-0.03	0.05	0.15	0.03	0.07	-0.03	0.12

PRCPTOT - Annual Total Wet-Day Precipitation

	A1	A2	A3	A4	A5	A6	A7	A8	A9	A10	A11	A12	A13	A14	A15	A16	A17	A18	A19
SOI	-0.06	-0.08	-0.14	-0.16	-0.03	-0.10	-0.06	-0.08	-0.13	-0.21	-0.14	-0.01	-0.03	-0.02	-0.09	-0.06	0.07	-0.07	-0.01
PDOI	-0.05	0.01	0.07	0.04	-0.02	0.03	-0.01	0.00	-0.04	0.03	-0.02	0.07	0.04	-0.05	0.19	0.12	-0.02	0.18	0.13
NAOI	0.01	-0.03	0.02	0.04	-0.03	-0.03	-0.19	0.04	-0.01	0.06	0.09	0.02	0.03	-0.05	0.10	0.05	-0.07	0.00	-0.04
AMOI	0.07	0.12	0.05	-0.02	0.01	0.01	0.04	-0.06	0.04	-0.07	-0.15	-0.12	-0.09	-0.08	-0.21	-0.17	-0.05	-0.11	-0.03

R10 - Number of Days with Precipitation Above 10 mm

	A1	A2	A3	A4	A5	A6	A7	A8	A9	A10	A11	A12	A13	A14	A15	A16	A17	A18	A19
SOI	-0.02	-0.01	-0.09	-0.17	-0.08	-0.12	-0.05	-0.08	-0.11	-0.21	-0.15	0.07	-0.02	-0.07	0.02	0.12	0.12	-0.02	0.02
PDOI	-0.19	-0.03	0.05	0.03	-0.03	0.00	0.01	-0.01	-0.04	0.02	0.00	0.07	0.09	-0.03	0.18	0.10	-0.02	0.18	0.14
NAOI	0.01	-0.05	-0.02	0.03	0.06	-0.04	-0.18	0.06	0.01	0.04	0.07	-0.02	-0.04	-0.08	0.00	0.05	-0.07	-0.08	0.07
AMOI	0.07	0.18	0.08	0.00	0.02	0.03	0.04	-0.02	0.00	-0.03	-0.07	-0.15	-0.10	-0.14	-0.19	-0.18	-0.05	-0.07	-0.09

R25 - Number of Days with Precipitation Above 25 mm

	A1	A2	A3	A4	A5	A6	A7	A8	A9	A10	A11	A12	A13	A14	A15	A16	A17	A18	A19
SOI	-0.03	-0.12	-0.09	-0.18	0.00	0.02	-0.11	0.01	-0.02	-0.13	-0.10	0.10	0.21	0.25	-0.06	-0.05	0.05	0.02	0.03
PDOI	-0.19	0.02	0.04	-0.09	-0.13	0.00	0.10	0.02	-0.02	-0.04	-0.13	-0.01	-0.12	-0.14	0.14	0.00	-0.01	0.15	0.07
NAOI	-0.10	-0.15	0.01	0.01	-0.04	-0.14	-0.24	-0.04	-0.08	0.01	-0.07	0.11	0.01	-0.09	0.15	0.06	-0.11	-0.02	-0.08
AMOI	0.33	0.38	0.04	0.10	-0.01	0.12	0.01	-0.02	0.16	0.04	-0.08	-0.31	-0.10	-0.02	-0.20	-0.24	-0.05	-0.08	-0.04

Table 5 - Correlation data between the oceanic oscillation indices (SOI, PDOI, NAOI and AMOI) and the climatic precipitation indices (R95p, R99p, SDII, RX1day e RX5day).

R95p - Very Wet Days

	A1	A2	A3	A4	A5	A6	A7	A8	A9	A10	A11	A12	A13	A14	A15	A16	A17	A18	A19
SOI	0.17	-0.07	-0.15	-0.10	0.04	0.04	-0.14	0.01	-0.08	-0.15	-0.11	0.05	0.17	0.29	-0.01	-0.04	0.11	-0.01	-0.01
PDOI	-0.22	0.01	0.10	-0.07	-0.11	-0.05	0.12	0.06	0.01	-0.03	-0.12	-0.01	-0.12	-0.17	0.09	0.05	-0.05	0.13	0.07
NAOI	-0.11	-0.17	0.10	0.01	-0.09	-0.18	-0.23	0.01	-0.06	0.00	-0.07	0.09	-0.05	-0.06	0.12	0.04	-0.16	0.01	-0.02
AMOI	0.31	0.41	-0.05	0.05	0.03	0.14	0.03	-0.05	0.12	0.06	0.00	-0.26	-0.06	0.00	-0.24	-0.23	-0.05	-0.09	-0.09

R99p - Extremely Wet Days

	A1	A2	A3	A4	A5	A6	A7	A8	A9	A10	A11	A12	A13	A14	A15	A16	A17	A18	A19
SOI	0.15	-0.16	-0.12	-0.02	0.12	0.12	-0.17	-0.02	-0.21	-0.07	-0.09	0.13	0.19	0.30	-0.04	-0.01	0.09	-0.14	-0.03
PDOI	-0.10	0.02	0.21	0.05	0.01	-0.03	0.11	0.14	0.12	-0.03	-0.09	-0.03	-0.14	-0.12	0.03	-0.01	-0.13	0.07	0.05
NAOI	0.00	-0.05	0.19	0.04	0.00	-0.04	-0.11	0.11	0.07	0.04	0.00	0.01	0.09	-0.15	0.08	-0.05	-0.01	0.15	0.02
AMOI	0.18	0.15	-0.13	0.01	-0.02	0.05	0.01	-0.13	0.09	0.09	0.04	-0.14	-0.12	0.00	-0.09	-0.12	-0.17	-0.08	-0.15

SDII - Simple Daily Intensity Index

	A1	A2	A3	A4	A5	A6	A7	A8	A9	A10	A11	A12	A13	A14	A15	A16	A17	A18	A19
SOI	0.13	-0.01	-0.10	-0.16	0.07	0.11	-0.03	0.01	-0.08	-0.16	-0.11	0.14	0.12	0.08	0.08	0.10	0.11	0.08	0.00
PDOI	-0.17	0.00	0.17	0.03	-0.10	-0.08	0.11	0.06	-0.01	-0.06	-0.05	-0.01	-0.06	-0.02	0.05	0.08	0.02	0.05	0.13
NAOI	-0.12	-0.10	0.11	0.06	-0.03	-0.10	-0.17	0.11	0.08	-0.02	-0.02	-0.07	-0.11	-0.11	0.11	-0.02	-0.08	0.03	-0.03
AMOI	0.33	0.39	0.02	0.16	0.18	0.17	0.03	-0.02	0.08	0.17	0.22	-0.18	-0.08	-0.09	-0.17	-0.24	-0.09	0.02	-0.04

RX1day - Max 1-day Precipitation Amount

	A1	A2	A3	A4	A5	A6	A7	A8	A9	A10	A11	A12	A13	A14	A15	A16	A17	A18	A19
SOI	-0.06	0.03	-0.07	-0.08	-0.01	-0.02	-0.07	-0.04	-0.06	-0.03	0.01	-0.03	0.00	0.00	-0.04	-0.08	-0.01	-0.01	-0.03
PDOI	0.13	0.07	0.04	0.05	0.09	0.07	0.07	0.03	0.05	0.07	0.03	0.06	0.01	0.06	0.08	0.11	0.08	0.09	0.11
NAOI	0.00	0.08	0.01	0.01	-0.03	-0.01	-0.01	0.03	-0.01	-0.01	0.01	0.02	0.07	-0.01	0.02	-0.02	0.00	0.02	0.03
AMOI	-0.08	-0.03	-0.09	-0.09	-0.05	-0.07	-0.05	-0.09	-0.04	-0.03	-0.09	-0.09	-0.05	-0.04	-0.14	-0.10	-0.07	-0.04	-0.10

RX5day - Max 5-day Precipitation Amount

	A1	A2	A3	A4	A5	A6	A7	A8	A9	A10	A11	A12	A13	A14	A15	A16	A17	A18	A19
SOI	-0.01	-0.01	-0.01	-0.02	0.00	0.01	-0.01	-0.01	-0.06	-0.08	0.00	-0.03	0.00	-0.02	-0.03	-0.04	0.02	-0.01	0.00
PDOI	0.12	0.09	0.01	0.02	0.05	0.08	0.05	0.00	0.05	0.05	0.05	0.07	0.05	0.07	0.09	0.13	0.06	0.11	0.11
NAOI	0.02	0.02	0.05	-0.02	-0.01	0.00	-0.06	0.04	0.01	-0.02	0.04	0.00	0.00	0.01	0.00	-0.03	0.01	0.02	0.01
AMOI	-0.02	-0.08	-0.12	-0.09	-0.11	-0.10	-0.03	-0.10	-0.07	-0.09	-0.09	-0.07	-0.05	-0.11	-0.08	-0.07	-0.08	-0.04	-0.04

In his study, Ferreira (2019) also identified the maximum number of consecutive dry days in the region in a strong La Niña event, which occurred in 1988. It was found that there is variability between the extreme precipitation rates in the Paraíba do Sul river basin. Even so, with regard to sensitivity to ENSO, for both negative and positive phases, the study identified a predominance of extreme events with frequent precipitation in the years in which El Niño occurred and a predominance of drought events in the years in which La Niña occurred.

However, the low values of correlation coefficients found suggest the existence of other mechanisms that govern the behavior of the trend of extreme precipitation indices in the region, such as anthropic factors and other climatic events. Examples of these phenomena are urban heat islands and changes in the position and intensity of the SASA, according to studies by Marengo et al. (2020) and Ribeiro (2020).

Table 4 summarizes the results of the analysis of search for correlation between the oceanic oscillation indices (SOI, PDOI, NAOI and AMOI) and the climatic precipitation indices (CDD, CWD, PRCPTOT, R10 and R25), calculated from the precipitation of the PSD-NOAA database, in each of the 19 grid points referring to the Paraíba do Sul river basin, for the period from 1938 to 2011. The values highlighted in blue and red indicate weak and moderate correlations, respectively.

Similarly, Table 5 condenses the results of the analysis of search for correlation between the oceanic oscillation indices (SOI, PDOI, NAOI and AMOI) and the climatic precipitation indices (R95p, R99p, SDII, RX1day e RX5day), calculated from the precipitation of the PSD-NOAA database, in each of the 19 grid points referring to the Paraíba do Sul river basin, for the period from 1938 to 2011. The values highlighted in blue and red indicate weak and moderate correlations, respectively.

3.3. Wavelets

Since no significant correlations were found between climatic extreme precipitation indices and oceanic indices, the Wavelet Technique was applied in order to verify the possible existence of different frequency patterns from the investigated correlations. Figure 4 illustrates the wavelet power spectrum for the precipitation levels observed in the Paraíba do Sul river basin. Through the analysis of the wavelet continuous spectrum for the climatic precipitation indices, the annual variability was verified (approximately 365 days), not only being present throughout the whole analysis period, but also revealing statistical significance. This behavior is attributed to the annual cycle of precipitation in the region, with dry southern winter and rainy summer (Brito et al., 2017; Brasiliense et al., 2020; Luiz-Silva et al., 2020).

Using the global spectrum, it was found that this annual variability was the one that occurred, on average, with greater power. Similarly, the variability with a period of around 5 days also showed statistical significance. In this region, this variability is associated with the passage of frontal systems during winter and the effect of SACZ during summer time (Dereczynski et al., 2009; Bonnet et al., 2018).

Corroborating the results obtained previously, there is no significant power in the low frequencies analyzed, commonly associated with oceanic phenomena, such as those obtained by Silva et al. (2010) for a hydrographic basin located in northeastern Brazil.

Figure 4 shows the wavelet power spectrum of precipitation for the Paraíba do Sul river hydrographic basin. The graph on the left shows the continuous spectrum. The hatched region represents the cone of influence, where edge effects become important. The black outlines mark the significant regions for the 95% confidence interval. On the right, in the graph of the same figure, the black line denotes the global spectrum and the dashed line, in red, represents the limit for the identification of statistically significant periodicities at the 5% level.

Figure 4 – Morlet wavelet power spectrum of Paraíba do Sul river basin precipitation. In the left panel, the black contour in wavelet spectrum indicates 95% confidence level against red noise and the cone of influence is shown by a darker shade. In the right panel, dashed curve indicates 95% confidence level and black line denotes the global wavelet power spectrum.

4. Conclusions

As observed by the results of the study, the eastern and northeastern regions of the Paraíba do Sul river hydrographic basin present trends of increase (i) in the total annual precipitation; (ii) in the number of very humid days; (iii) in the maximum amount of 1-day precipitation; (iv) in the maximum amount of precipitation in 5 consecutive days, and decreasing trends (v) in the number of consecutive dry days. On the other hand, the west and southwest regions, show decreasing trends in the total annual precipitation rate and in the number of very humid days, but a trend towards an increase in the maximum amount of precipitation in 5 consecutive days. The central region of the basin shows a transition zone behavior of the studied indices. All the patterns described for the different sectors of the basin indicate that intense rainfall is concentrated in a fewer days followed by periods of drought, which is an indication that the temporal distribution of precipitation in the region is changing. Similar signs of trends in extreme precipitation indices, especially in heavy rain events, are in line with the results obtained by other researchers in Brazil (Carvalho et al., 2014; Silva and Dereczynski, 2014; Zilli et al., 2017; Ávila et al., 2020; Marengo et al., 2020).

Correlation analyzes show that most ocean oscillation indices have a very weak correlation with the extreme precipitation indices. Therefore, it is not possible to associate droughts (negative anomalies) or excess rain (positive anomalies) to the occurrence of the oceanic phenomena studied. Thus, after using the wavelet transform to decompose precipitation in the time-frequency domain, no significant power is observed in the low frequencies commonly associated with oceanic phenomena, a fact that corroborates the results of the investigated correlation analyzes.

Following this study, further developments of the work are proposed: seasonal study of the extreme precipitation indices in the region and investigation of the influence of the dynamic conditions of the atmosphere on these indices (eg: intensity and location of systems, such as SACZ and SASA).

Declarations

Funding

This work was supported by National Electric Energy Agency (Aneel) and Light Energia S/A (Grant numbers R&D Light/Aneel project 5161-0016 / 2019, Contract 4500428146).

Competing Interests

The authors have no relevant financial or non-financial interests to disclose.

Author Contributions

All authors contributed to the study conception and design. Material preparation, data collection and analysis were performed by all authors (see credit taxonomy below). The first draft of the manuscript was

written by Mônica Senna and all authors commented on previous versions of the manuscript. All authors read and approved the final manuscript.

Credit Taxonomy:

Mônica Senna

Conceptualization, Data curation, Formal analysis, Investigation, Methodology, Software, Supervision, Validation, Visualization, Writing – original draft, Writing – review & editing

Gutemberg França

Conceptualization, Formal analysis, Funding acquisition, Investigation, Project administration, Resources, Supervision, Validation, Writing – review & editing

Matheus Pereira

Data curation, Formal analysis, Investigation, Methodology, Software, Visualization

Mauricio Soares da Silva

Formal analysis, Investigation, Methodology, Software, Validation, Visualization, Writing – review & editing

Enio Souza

Funding acquisition, Investigation, Project administration, Resources, Supervision, Validation, Writing – review & editing

Ian Dragaud

Formal analysis, Investigation, Methodology, Software, Validation, Visualization, Writing – review & editing

Lucio Souza

Investigation, Methodology, Validation, Writing – review & editing

Nilton Moraes

Investigation, Methodology, Validation, Writing – review & editing

Vinicius Almeida

Investigation, Validation

Manoel Almeida

Investigation, Validation

Mauricio Frota

Funding acquisition, Project administration, Resources, Supervision, Writing – review & editing

Afonso Araujo

Investigation, Validation

Karine Cardozo

Software, Visualization

Lude Viana

Conceptualization, Data curation, Funding acquisition, Project administration, Resources, Supervision, Writing – review & editing

Data Availability

The data that support the findings of this study are available from South American Precipitation data provided by the NOAA/OAR/ESRL PSL, Boulder, Colorado, USA, from their Web site at https://psl.noaa.gov/data/gridded/data.south_america_precip.html. This data set is for general public distribution.

Acknowledgments

Thanks are due (i) to the National Electric Energy Agency (Aneel) and to the concessionaire of Energy Light Energia S/A, for the financial assistance granted within the scope of the R&D Light/Aneel project 5161-0016 / 2019, Contract 4500428146 and (ii) to the Coordination for the Improvement of Higher Education Personnel (CAPES/ Ministry of Education of Brazil), for institutional support (Financing Code 001) to the Graduate Programs of the universities involved in the development of the R&D project.

References

1. ABOU RAFEE, S., FREITAS, E., MARTINS, J. et al. (2020) Spatial trends of extreme precipitation events in the Paraná river basin. J Appl Meteorol Climatol 59:443–454. https ://doi.org/10.1175/JAMC-D-19-0181.1
2. ADEPITAN, J. O., & FALAYI, E. O. (2019) Variability changes of some climatology parameters of Nigeria using wavelet analysis. Scientific African, 2, pp. 1-11.
3. AGÊNCIA NACIONAL DE ÁGUAS E SANEAMENTO BÁSICO (ANA) (2010) Previsão de eventos críticos na bacia do rio Paraíba do Sul, R 02 - Coleta de Dados. Engecorps, 285 p.

4. ALEXANDER, L. et al. (2006) Global observed changes in daily climate extremes of temperature and precipitation. J Geophys Res 111(D5): 1-22.
5. ÁVILA, A., JUSTINO, F., AARON, W., BROMWICH, D. & AMORIM, M. (2016) Recent precipitation trends, flash floods and landslides in southern Brazil. Environ Res Lett 11(11): 1-13.
6. ÁVILA, A. D.; JUSTINO, F.; LINDEMANN, D. S.; RODRIGUES, J. M. & FERREIRA, G. R. (2020) Climatological aspects and changes in temperature and precipitation extremes in Viçosa-Minas Gerais. Anais da Academia Brasileira de Ciências, 92(2).
7. BONNET, S. M., DERECZYNSKI, C. P., & NUNES, A. (2018) Caracterização sinótica e climatológica de eventos de chuva pós-frontal no Rio de Janeiro. Revista Brasileira de Meteorologia, 33(3), 547-557.
8. BRASILIENSE, C. S., DERECZYNSKI, C. P., SATYAMURTY, P., CHOU, S. C., DA SILVA SANTOS, V. R., & CALADO, R. N. (2018) Synoptic analysis of an intense rainfall event in Paraíba do Sul river basin in southeast Brazil. Meteorological Applications, 25(1), 66-77.
9. BRASILIENSE, C. S.; DERECZYNSKI, C. P.; SATYAMURTY, P.; CHOU, S. C. & CALADO, R. N. (2020) Climatologias da Temperatura do Ar e da Precipitação na Bacia do Rio Paraíba do Sul, Região Sudeste do Brasil. Anuário do Instituto de Geociências, 43(1).
10. BRITO, T. T., OLIVEIRA-JÚNIOR, J. F., LYRA, G. B., GOIS, G., & ZERI, M. (2017) Multivariate analysis applied to monthly rainfall over Rio de Janeiro state, Brazil. Meteorology and Atmospheric Physics, 129(5), 469-478.
11. CAI, W., P. H. WHETTON, AND D. J. KAROLY (2003) The response of the Antarctic oscillation to increasing and stabilized atmospheric CO2, J. Clim., 16, 1525 – 1538.
12. CARDOSO, A.O.; CATALDI, M. (2012) Relações de índices climáticos e vazão de rios no Brasil. In: Congresso Brasileiro de Meteorologia, 17., 2012, Gramado. Anais... Rio de Janeiro: SBMET.
13. CARPENEDO, C.B.; AMBRIZZI, T. (2020) Anticiclone Subtropical do Atlântico Sul Associado ao Modo Anular Sul e Impactos Climáticos no Brasil. Revista Brasileira de Meteorologia, v. 35, n. 4, p. 605-613.
14. CARVALHO, J.R.P., ASSAD, E.D., DE OLIVEIRA, A.F. & PINTO, H.S. (2014) Annual maximum daily rainfall trends in the Midwest, Southeast and Southern Brazil in the last 71 years. Weather Clim Extrem 5(1): 7-15.
15. CASTAÑEDA, M.E.; BARROS, V. R. (1994) Las tendencias de la precipitacion en el Cono Sur de America al leste de los Andes. Meteorologica, 19, 23-2.
16. CATALDI, M.; ASSAD, L.P.F.; TORRES JUNIOR, A.R.; ALVES, J.L.D. (2010) Estudo da influência das anomalias da TSM do Atlântico Sul extratropical na região da Confluência Brasil-Malvinas no regime hidrometeorológico de verão do Sul e Sudeste do Brasil. Rev. Bras. Meteorol. 25, 513–524. https://doi.org/10.1590/s0102-77862010000400010.
17. CEIVAP (2006) Plano de Recursos Hídricos da Bacia do Rio Paraíba do Sul - Resumo.
18. CHADWICK R, GOOD P, MARTIN G & ROWELL DP. (2016) Large rainfall changes consistently projected over substantial areas of tropical land. Nat Clim Chang 6(2): 177-181.

19. CHIESSI, C. M.; MULITZA, S.; PATZOLD, J.; WEFER, G.; MARENGO, J. A. (2009) Possible impact of the Atlantic Multidecal Oscillation on the South American Summer monsoon. Geophysical Research letters, v. 36, L21707, p. 5.
20. COELHO, C.A.S.; DE OLIVEIRA, C.P.; AMBRIZZI, T. et al. (2016) The 2014 southeast Brazil austral summer drought: regional scale mechanisms and teleconnections. Clim Dyn 46, 3737–3752. https://doi.org/10.1007/s00382-015-2800-1.
21. COSTA, A.S.; DOS SANTOS, N.A.; BRAGA, C.C. (2016) Rainfall diagnosis in different time scales in Maranhão using the wavelet transform. Journal of Hyperspectral Remote Sensing, 6 (6), 295-304.
22. DERECZYNSKI, C.P.; OLIVEIRA, J.S.; MACHADO, C.O. (2009) Climatologia da precipitação no município do Rio de Janeiro. Rev. bras. meteorol., 24 (1), 24-38.
23. DERECZYNSKI, C.P.; LUIZ SILVA, W.; MARENGO, J.A. (2013) Detection and projections of climate change in Rio de Janeiro, Brazil. Am. J. Clim. Change 2: 25–33, doi: 10.4236/ajcc.2013.21003.
24. DEUSDARÁ-LEAL, K.R.; CUARTAS, L.A.; ZHANG, R.; MOHOR, G.S.; DE CASTRO CARVALHO, L.V.; NOBRE, C.A.; MENDIONDO, E.M.; BROEDEL, E.; SELUCHI, M.E. & DOS SANTOS ALVALÁ, R.C. (2020) Implications of the New Operational Rules for Cantareira Water System: Re-Reading the 2014-2016 Water Crisis. Journal of Water Resource and Protection, 12, 261-274. https://doi.org/10.4236/jwarp.2020.124016.
25. DONAT, M.G.; LOWRY, A.L.; ALEXANDER, L.V.; O'GORMAN, P.A.; MAHER, N. (2016) More extreme precipitation in the world's dry and wet regions. Nature Climate Change, 6: 508-513.
26. DONG, S.; SUN, Y.; LI, C.; ZHANG, X.; MIN, S.K.; KIM, Y.H. (2021) Attribution of Extreme Precipitation with Updated Observations and CMIP6 Simulations. Journal of Climate, 34: 871-881.
27. ECHER, M.P.S.; ECHER, E.; NORDEMANN, D.J.; RIGOZO, N.R.; PRESTES, A. (2008) Wavelet analysis of a centennial (1895–1994) southern Brazil rainfall series (Pelotas, 31°46'19"S; 52°20'33"W). Climatic Change, 87(3-4): 489-497.
28. FERREIRA, G. R. (2019) Eventos extremos de precipitação nas bacias hidrográficas dos rios Doce e Paraíba do Sul. Dissertação (Mestrado em Meteorologia Aplicada) - Universidade Federal de Viçosa / Gabriela Regina Ferreira. – Viçosa, MG, 47p.
29. FYFE, J. C., G. J. BOER, AND G. M. FLATO (1999) The Arctic and Antarctic oscillations and their projected changes under global warming, Geophys.Res. Lett., 26, 1601 – 1604.
30. GARCIA, S. R.; KAYANO, M. T. (2008) Climatological aspects of Hadley, Walker and monsoon circulations in two phases of the Pacific Decadal Oscillation. Theoretical and Applied Climatology, v. 91, p. 117–127.
31. GROISMAN, P.Y.; KNIGHT, R.W.; EASTERLING, D.R.; KARL, T.R.; HEGERL, G.C.; RAZUVAEV, V.A.N. (2005) Trends in intense precipitation in the climate record. Journal of Climate, v.18, p. 1326–1350.
32. HAIR, J.F.; ANDERSON, R.E.; TATHAM, R.L.; BLACK, W.C. (2005) Análise multivariada de dados. 5.ed. Porto Alegre: Bookman, 593p.
33. HINKLE, D.E.; WIERSMA, W.; JURS, S.G. (2003) Applied Statistics for the Behavioral Sciences. 5th ed. Boston: Houghton Mifflin. 792 p.

34. IPCC - INTERGOVERNMENTAL PANEL ON CLIMATE CHANGE (2018) Summary for Policymakers. In: Global Warming of 1.5°C. An IPCC Special Report on the impacts of global warming of 1.5°C above pre-industrial levels and related global greenhouse gas emission pathways, in the contexto of strengthening the global response to the threat of climate change, sustainable development, and efforts to eradicate poverty, Masson-Delmotte V ET AL (eds). World Meteorological Organization, Geneva, Switzerland, p. 1-32.
35. KAYANO, M. T.; ANDREOLI, R. V. (2007) Relation of South American summer rainfall interannual variations with the Pacific Decadal Oscillation. Int. J. Climatology, vol.27, n.4, p. 531-540.
36. KNIGHT, J. R.; ALLAN, R. J.; FOLLAND, C. K.; VELLINGA, M.; MANN, M. E. (2005) A signature of persistent natural thermohaline circulation cycles in observed climate. Geophysical Research Letters, v. 32, L. 20708, doi: 10.1029/2005GL024233.
37. KREPPER, C.M.; SEQUEIRA, M.E. (1998) Low frequency variability of rainfall in southeastern South America. Theor. Appl. Climatol., 61, 19-28.
38. KUSHNER, P. J., I. M. HELD, AND T. L. DELWORTH (2001) Southern Hemisphere atmospheric circulation response to global warming, J. Clim., 14, 2238–2249.
39. LIEBMANN, B., ALLURED, D. (2005) Daily precipitation grids for South America. Bull. Am. Meteorol. Soc. 86: 1567–1570.
40. LONGUEVILLE, F.D.; HOUNTONDJI, Y.C.; KINDO, I.; GEMENNE, F.; OZER, P. (2016) Long-term analysis of rainfall and temperature data in Burkina Faso (1950–2013). International Journal of Climatology, 36 (13): 4393-4405.
41. LOPES, L. G. (2018) Mudança na disponibilidade hídrica associada às mudanças climáticas e no uso e cobertura da terra na região paulista da bacia do rio Paraíba do Sul. Dissertação (Mestrado em Engenharia de Biossistemas), Universidade Federal Fluminense, Niterói, RJ/Brasil, 85 p.
42. LUIZ-SILVA, W., OSCAR-JÚNIOR, A. C., CAVALCANTI, I. F. A., & TREISTMAN, F. (2020) An Overview of Precipitation Climatology in Brazil: Space-Time Variability of Frequency and Intensity associated with Atmospheric Systems. Hydrological Sciences Journal.
43. MARENGO, J. A. (2006) On the hydrological cycle of the Amazon basin: a historical review and current state-of-the-art. Revista Brasileira de Meteorologia, v. 21, p. 1-19.
44. MARENGO, J. A.; ALVES, L. M. (2005) Tendências hidrológicas da Bacia do Rio Paraíba do Sul. Revista Brasileira de Meteorologia, Rio de Janeiro, v. 20, n. 2, p. 215- 226.
45. MARENGO, J. A.; ALVES, L. M.; VALVERDE, M. A.; LABORBE, R.; ROCHA, R. P. (2007) Eventos extremos em cenários regionalizados de clima no Brasil e América do Sul para o Século XXI: Projeções de clima futuro usando três modelos regionais. Relatório 5, Ministério do Meio Ambiente (MMA), Secretaria de Biodiversidade e Florestas (SBF), Diretoria de Conservação da Biodiversidade (DCBio). Mudanças Climáticas Globais e Efeitos sobre a Biodiversidade - Subprojeto: Caracterização do clima atual e definição das alterações climáticas para o território brasileiro ao longo do século XXI. Brasília.

46. MARENGO, J.A., ALVES, L.M., AMBRIZZI, T., YOUNG, A., BARRETO, N.J.C. & RAMOS, A.M. (2020) Trends in extreme rainfall and hydrogeometeorological disasters in the Metropolitan Area of São Paulo: a review. Ann N Y Acad Sci 1-16.
47. MARENGO, J.A.; VALVERDE, M.C.; OBREGON, G.O. (2013) Observed and projected changes in rainfall extremes in the Metropolitan Area of São Paulo. Clim. Res., 57(1): 61-72.
48. MARSHALL, G.J.; STOTT, P.A.; TURNER, J.; CONNOLLEY, W.M.; KING, J.C.; LACHLAN-COPE, T.A. (2004) Causes of exceptional atmospheric circulation changes in the Southern Hemisphere. Geophysical Research Letters, v. 31, n. 14.
49. MIN, S.K., ZHANG, X., ZWIERS, F. W. & HEGERL, G. C. (2011) Human contribution to more-intense precipitation extremes. Nature, 470: 378–381.
50. MINUZZI, R.B.; SEDIYAMA, G.C.; COSTA, J.M.N.; VIANELLO, R.L. (2006) Influência do fenômeno climático El Niño no período chuvoso da região sudeste do Brasil. Geografia, 15 (2), 5–19.
51. MINUZZI, R.B.; SEDIYAMA, G.C.; COSTA, J.M.N.; VIANELLO, R.L. (2006) Influência da La Niña na estação chuvosa da região sudeste do Brasil. Revista Brasileira de Meteorologia, 22 (3), 345–353.
52. MORETTIN, P.A. (1999) Ondas e Ondaletas: Da Análise de Fourier à Análise de Ondaletas. São Paulo, Editora da Universidade de São Paulo, 276p.
53. NÍMER, E. (1989) Climatologia do Brasil. 2ª ed. Rio de Janeiro: IBGE Departamento de Recursos Naturais e Estudos Ambientais.
54. NOBRE, P.; SHUKLA, J. (1996) Variations of sea surface temperature, wind stress and rainfall over the tropical Atlantic and South America. Journal of Climate, v. 9, n.10, p. 2464–2479.
55. OLIVEIRA-JÚNIOR, J.F.; GOIS, G.; TERASSI, P.M.B.; JUNIOR, C.A.S.; BLANCO, C.J.C.; SOBRAL, B.S.; GASPARINI, K.A.C. (2018) Drought severity based on the SPI index and its relation to the ENSO and PDO climatic variability modes in the regions North and Northwest of the State of Rio de Janeiro–Brazil. Atmos. Res., 212, 91–105. https://doi.org/10.1016/j.atmosres.2018.04.022.
56. OSCAR JR., A. C. S. (2015) Extremos atmosféricos e desastres hidrometeorológicos em Duque de Caxias (RJ). Revista Brasileira de Climatologia, v. 17, p. 189-205.
57. REBOITA, M.S.; AMBRIZZI, T.; DA ROCHA, R.P. (2009) Relationship between the southern annular mode and Southern Hemisphere atmospheric systems. Revista Brasileira de Meteorologia, 24 (1), 48-55.
58. REBOITA, M.S.; OLIVEIRA, D.M.; FREITAS, C.H. et al. (2015) Anomalias dos Padrões Sinóticos da Atmosfera na América do Sul nos Meses de Janeiros de 2014 e 2015. Revista Brasileira de Energias Renováveis, 4, 1-12.
59. REBOITA, M.S.; AMBRIZZI, T.; SILVA, B.A.; PINHEIRO, R.F. & DA ROCHA, R.P. (2019) The South Atlantic Subtropical Anticyclone: Present and Future Climate. Front. Earth Sci. 7:8. doi: 10.3389/feart.2019.00008.
60. REGOTO, P.; DERECZYNSKI, C.; SILVA, W. L.; SANTOS, R.; CONFALONIERI, U. (2018) Tendências de Extremos de Precipitação para o Estado do Espírito Santo. Anuário do Instituto de Geociências – UFRJ, v. 41, p. 365-381.

61. RIBEIRO, E. M. (2020) Variabilidade de baixa frequência, teleconexões e seus efeitos sobre o regime de chuva e vazão do Brasil. Dissertação (Mestrado em Engenharia de Biossistemas), Universidade Federal Fluminense, Niterói, RJ/Brasil, 80 p.
62. ROBERTSON, A. W.; MECHOSO, C.R. (1998) Interannual and decadal cycles in river flows of southeastern South American. J. Climate, 11, 2570-2581.
63. SANTOS, C. A. C.; BRITO, J. I. B.; RAMANA RAO, T. V.; MENEZES, H. E. A. (2009) Tendências dos índices de precipitação no Estado do Ceará. Revista Brasileira de Meteorologia, v. 24, p. 39-47.
64. SANTOS, I.; REBOITA, M. S.; FRANCO, N. (2011) Uma avaliação preliminar do controle dinâmico dos padrões globais de teleconexões. In: Simpósio Internacional de Climatologia, 2011, João Pessoa. Mudanças Climáticas e os seus Impactos em Áreas Urbanas.
65. SILVA, D. F.; SOUZA, F. A. S.; KAYANO, M.T. (2010) Análise da Influência das Multi-Escalas Temporais na Precipitação da Bacia Hidrográfica do Rio Mundaú Através do IAC e Ondeletas: Baixo Mundaú. UNOPAR Cient. Exatas Tecnol., Vol. 9, Nº 1, 19-26.
66. SILVA, G.B.; AZEVEDO, P.V. (2008) Índices de tendências de mudanças climáticas no Estado da Bahia. Engenharia Ambiental: Pesquisa e Tecnologia, Vol. 5, Nº 3.
67. SILVA, W. L.; DERECZYNSKI, C. P. (2014) Caracterização Climatológica e Tendências Observadas em Extremos Climáticos no Estado do Rio de Janeiro. Anuário do Instituto de Geociências – UFRJ, v. 37, p. 123-138.
68. SIQUEIRA, A. H. B. (2012) Variabilidade do clima da América do Sul e sua relação com os índices oceânicos e atmosféricos. 79 f. Dissertação (Mestrado em Meteorologia) –Universidade Federal de Alagoas.
69. SOBRAL, B.S.; OLIVEIRA-JÚNIOR, J.F.D.; GOIS, G.; PEREIRA-JÚNIOR, E.R.; TERASSI, P.M.B.; MUNIZ-JÚNIOR, J.G.R.; LYRA, G.B.; ZERI, M. (2019) Drought characterization for the state of Rio de Janeiro based on the annual SPI index: trends, statistical tests and its relation with ENSO. Atmospheric Research, 220, 141–154. https://doi.org/10.1016/j.atmosres.2019.01.003.
70. SOUZA, W. M; AZEVEDO, P. V. (2012) Índices de Detecção de Mudanças Climáticas Derivados da Precipitação Pluviométrica e das Temperaturas em Recife-PE. Revista Brasileira de Geografia Física, 01, 143- 159.
71. STONE, D. A., A. J. WEAVER, AND R. J. STOUFFER (2001) Projection of climate change onto modes of atmospheric variability, J. Clim., 14, 3551 – 3565.
72. SUN, X.; COOK, K.H.; VIZY, E.K. (2017) The South Atlantic subtropical high: Climatology and interannual variability. Journal of Climate, v. 30, n. 9, p. 3279-3296.
73. TEIXEIRA, M.S. & SATYAMURTY, P. (2011) Trends in the frequency of intense precipitation events in Southern and southeastern Brazil during 1960-2004. J Clim 24(7): 1913-1921.
74. TORRENCE, C.; COMPO, G.P.A. (1998) Practical Guide to Wavelet Analysis. Bulletin of the American Meteorological Society, 79: 61-78.
75. VALVERDE, M. C.; MARENGO, J. A. (2014) Extreme Rainfall Indices in the Hydrographic Basins of Brazil. Open Journal of Modern Hydrology, v. 4, p. 10-26.

76. VITORINO, M.I.; SILVA DIAS, P.L.; FERREIRA, N.J. (2006) Observational study of the seasonality of the submonthly and intraseasonal signal over the tropics. Meteorology and Atmospheric Physics, 93: 17-35.
77. YOU, Q.; KANG, S.; AGUILAR, E.; PEPIN, N.; FLÜGEL, W.A.; YAN, Y.; XU, Y.; ZHANG, Y.; HUANG, J. (2011) Changes in daily climate extremes in China and their connection to the large scale atmospheric circulation during 1961–2003. Climate Dynamics, 36: 2399-2417.
78. ZHANG, X.; YANG, F. (2004) RClimDex (1.0) – User Manual. Climate Research Branch Environment. Canada Downsview.
79. ZHANG, X., WAN, H., ZWIERS, F.W., HEGERL, G.C. & MIN, S.K. (2013) Attributing intensification of precipitation extremes to human influence. Geophys. Res. Lett., 40: 5252–5257.
80. ZILLI, M.T., CARVALHO, L.M.V., LIEBMANN, B. & SILVA DIAS, M.A. (2017) A comprehensive analysis of trends in extreme precipitation over southeastern coast of Brazil. Int J Climatol 37(5): 2269-2279.

Figures

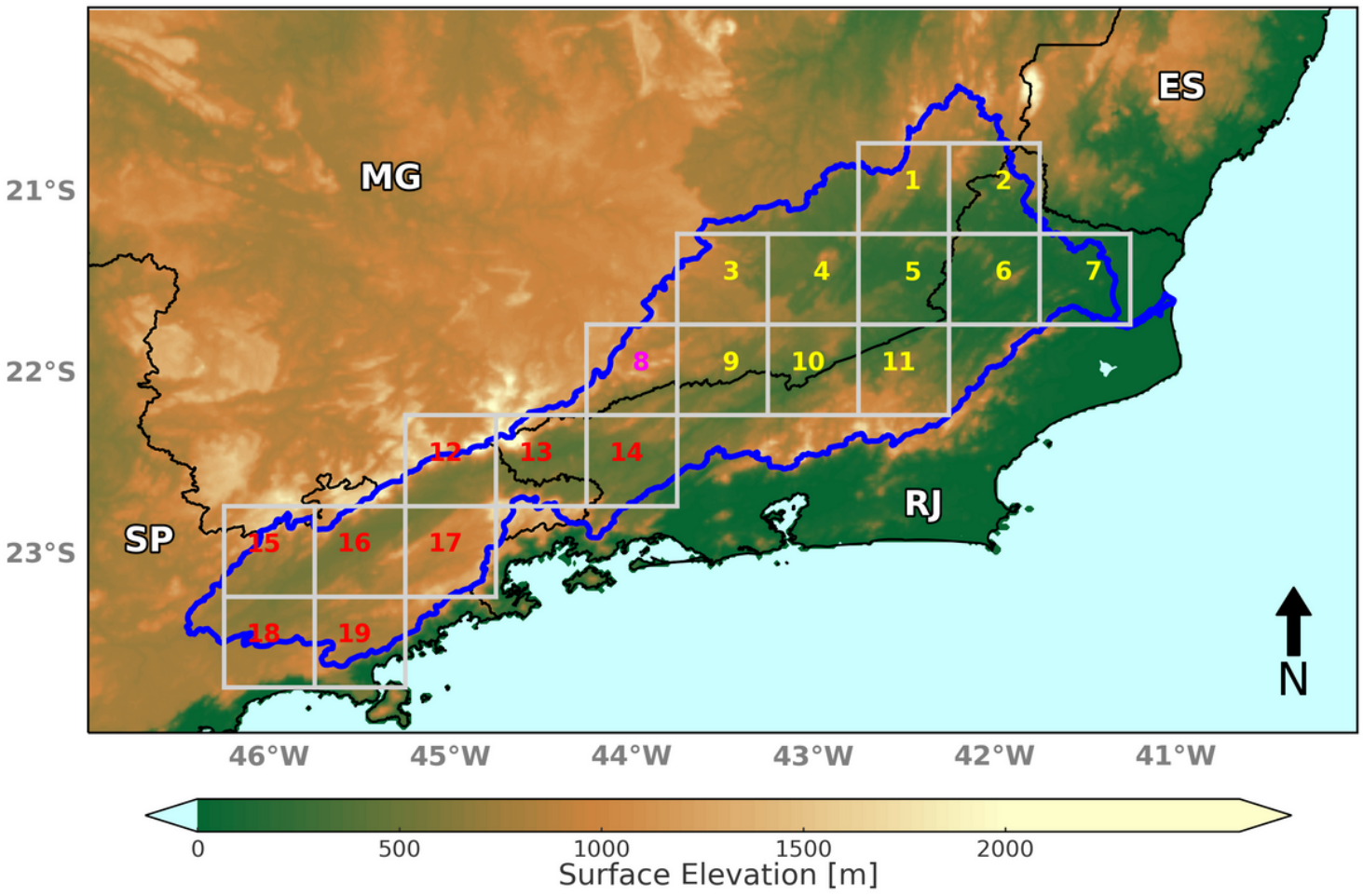

Figure 1

Paraíba do Sul river basin (delimited by a blue line), and its 19 grid points referring to the precipitation database used. The yellow grid points represent the northeast areas (1 to 7 and 9 to 11), the pink one the northwest (8), and the red points the southwest areas of the basin (12 to 19).

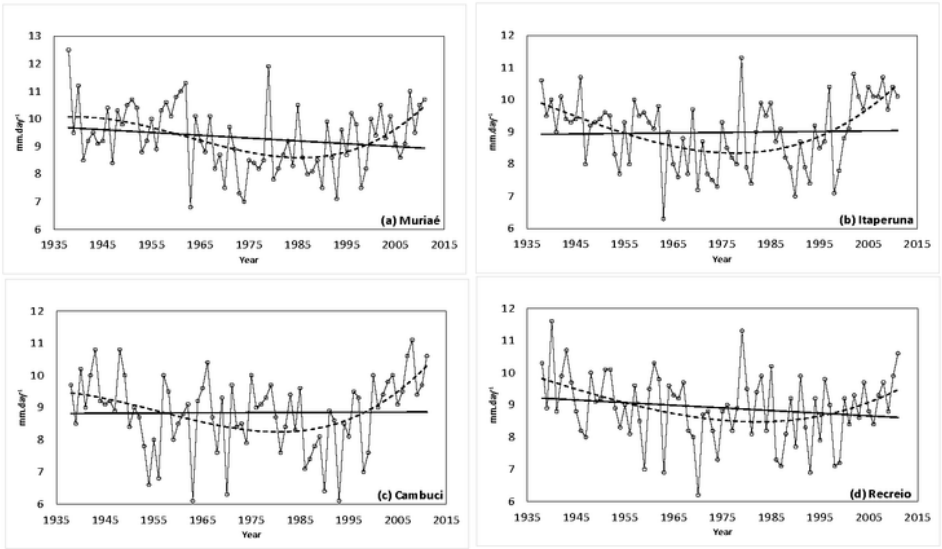

Figure 2

Linear (solid line) and non-linear (dashed line) trends of the SDII index, whose locations are indicated in Figures (2a - 2d), from 1938 to 2011.

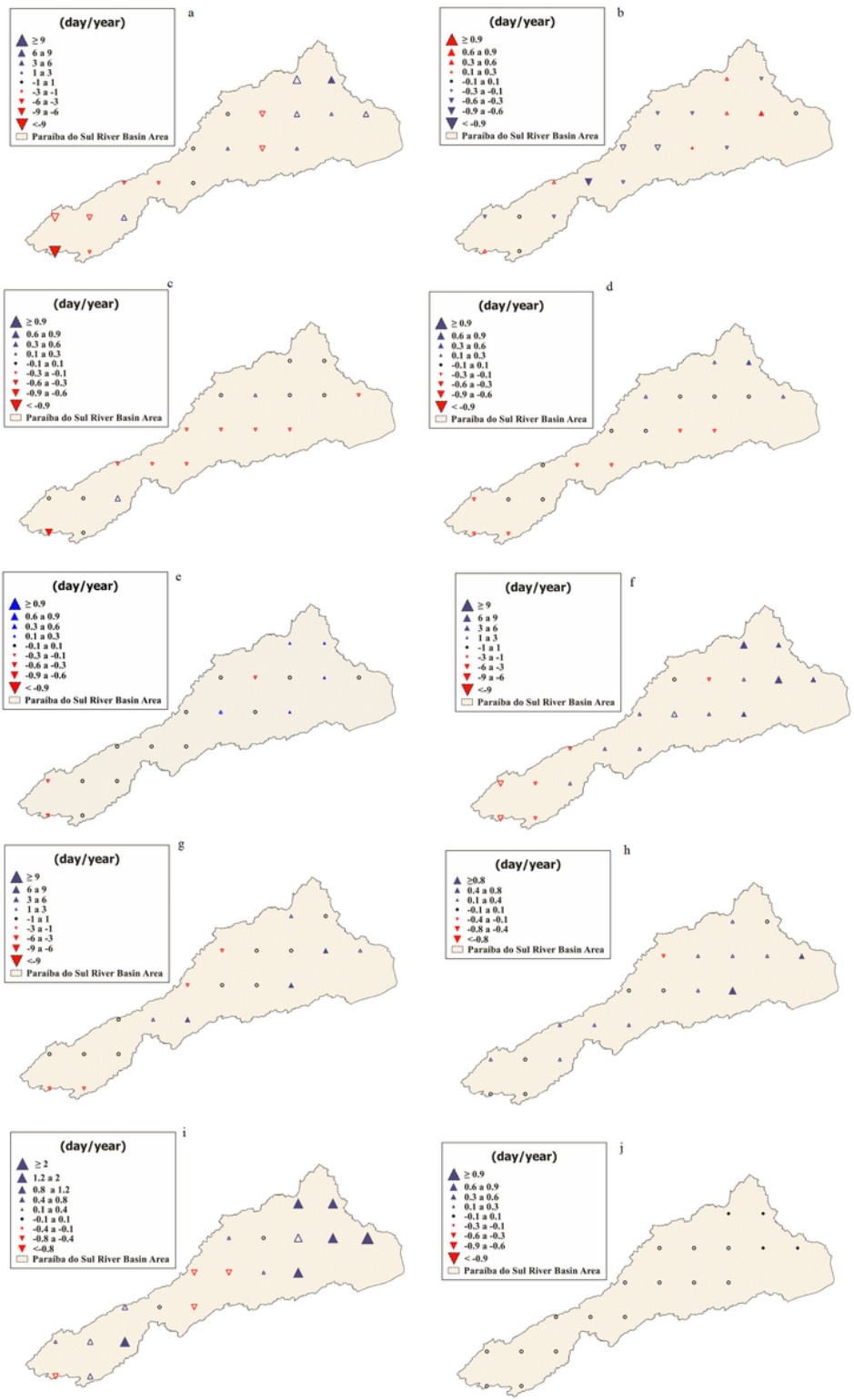

Figure 3

Spatial distribution of trends in the PRCPTOT index [mm/year] (a), CDD [day/year] (b), CWD [day/year] (c), R10 [day/year] (d), R25 [day/year] (e), R95p [mm/year] (f), R99p [mm/year] (g), RX1day [mm/year] (h), RX5day [mm/year] (i), and SDII [mm/day] (j) for the period from 1982 to 2011 in the Paraíba do Sul river basin.

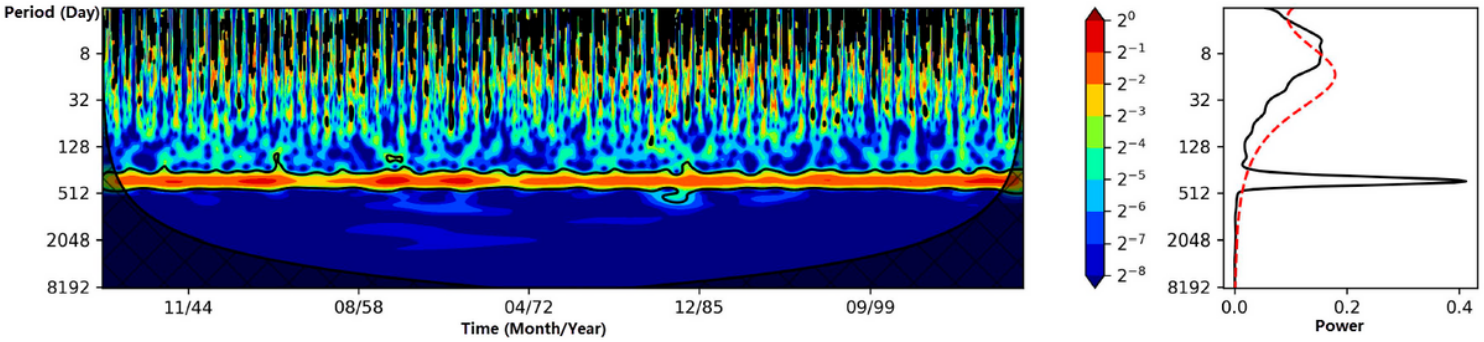

Figure 4

Morlet wavelet power spectrum of Paraíba do Sul river basin precipitation. In the left panel, the black contour in wavelet spectrum indicates 95% confidence level against red noise and the cone of influence is shown by a darker shade. In the right panel, dashed curve indicates 95% confidence level and black line denotes the global wavelet power spectrum.